Phyton-
International Journal of
Experimental Botany

Tech Science Press

http://doi.org/10.32604/phyton.2026.083772

ARTICLE

Functional Characterization of LsMYB1, a Positive Regulator of Anthocyanin Biosynthesis in Lettuce

Xuebing Zhu[1,2], Yongqiang Jiang[1,2], Wei Li[1,2], Lihui Wang[1,2] and Xuemei Sun[1,2,*]

[1]Academy of Agriculture & Forestry, Qinghai University, Xining, China
[2]Laboratory for Research and Utilization of Germplasm Resources in Qinghai Tibet Plateau, Qinghai University, Xining, China
*Corresponding Author: Xuemei Sun. Email: sunxuemei1008@163.com

Received: 10 April 2026; Accepted: 04 June 2026; Published: 30 July 2026

ABSTRACT: Although transcriptional regulators of anthocyanin biosynthesis have been studied in many crops, the regulatory network controlling the purple leaf trait in lettuce (*Lactuca sativa* L.) remains incompletely understood. Our previous transcriptome analysis identified *LsMYB1*. This study further carried out the cloning and structural feature analysis of the *LsMYB1* gene, and systematically verified its function using the tobacco heterologous overexpression system and CRISPR/Cas9 gene editing technology. Sequence analysis revealed a structural difference between the two alleles: the *LsMYB1* allele in the purplecultivar contains two introns and three exons, whereas the allele in the greencultivar comprises only a single exon. Overexpression of the purple-associated *LsMYB1* allele in tobacco induced anthocyanin accumulation and purple pigmentation. CRISPR/Cas9-mediated mutagenesis of *LsMYB1* in lettuce resulted in reduced anthocyanin content and loss of purple color in most leaf areas. These results confirmsthat LsMYB1 is a regulator of anthocyanin biosynthesis in leaf lettuce. This study also highlights the potential role of allelic structural variation in trait diversification and provides a candidate gene for breeding lettuce with enhanced anthocyanin content.

KEYWORDS: Leaf lettuce; anthocyanin; MYB; genetic transformation; CRISPR/Cas9

1 Introduction

Lettuce (*Lactuca sativa* L.), a member of the Asteraceae family originating from the Mediterranean region [1], has two primary morphological types: stem lettuce and leaf lettuce. Leaf lettuce is consumed for its tender leaves, which contain vitamin C, vitamin E, folate, polyphenols, and dietary fiber [2,3]. It is cultivated worldwide as an ingredient in vegetable salads and fast food. Leaf lettuce shows diverse coloration from green to purple [4]. Purple pigmentation results from anthocyanin accumulation, which provides health benefits—including anti-inflammatory effects and reduction of blood glucose and blood pressure [5–7]—and also enhances plant tolerance to environmental stress [8–10].

In lettuce, anthocyanin biosynthesis is regulated by both environmental factors and genetic determinants [11,12]. Different wavelengths of light affect anthocyanin accumulation, blue light enhances anthocyanin pigmentation compared with white light and red light [10,13,14]. In addition, Different light intensities have an effect on anthocyanin biosynthesis [15]. Under different light intensities (40 and 100 $\mu mol \cdot m^{-2} \cdot s^{-1}$), differential expression was observed in seven structural genes involved in anthocyanin biosynthesis (*CHS*, *CHI*, *F3H*, *F3'H*, *DFR*, *ANS*, *3GT*), two anthocyanin transporter genes (*arGST* and *MATE*), as well as the anthocyanin regulatory genes (*MYB* and *bHLH*) [14]. A locus controlling leaf color, designated

Copyright © 2026 The Authors. Published by Tech Science Press. This work is licensed under a Creative Commons Attribution 4.0 International License, which permits unrestricted use, distribution, and reproduction in any medium, provided the original work is properly cited.

RLL1, was identified within the interval of 335.69–337.92 Mb on lettuce chromosome 5. This locus contains a gene encoding a *bHLH* transcription factor, and a 5-bp deletion in its seventh exon results in green leaf color. Similarly, a locus encoding a *MYB* transcription factor, designated RLL2, was identified on chromosome 5 and exists in three copies (RLL2A, RLL2B, and RLL2C). Among these, RLL2A, which corresponds to the RLL2 gene, promotes anthocyanin accumulation in lettuce. RLL2B also promotes anthocyanin accumulation when highly expressed. On chromosome 4, a locus designated RLL3 encodes an *R3-MYB* gene. Two single nucleotide polymorphisms (SNPs) within its coding sequence (CDS)—G/A and G/C—result in amino acid substitutions (C42Y and W52S), leading to a shift in leaf color from green to red [16]. Additionally, six genes were found to be associated with leaf color and differentially expressed between green and red lettuce cultivars: *LG1_162414* (chr1), *GST* (chr3), *CAD* (chr4), *MYB113* (chr5), *bHLH42* (chr5), and *ANS* (chr9). Notably, *CAD* transcript levels were higher in green lettuce than in red lettuce, suggesting that *CAD* may act as a negative regulator of anthocyanin [17]. In lettuce, leaf color can also be variegated—green leaves dotted with red spots, this variegation stems from an "AT" repeat in the promoter of RLL2A, which encodes a *MYB* transcription factor [18]. Although several genes involved in anthocyanin biosynthesis have been identified in lettuce, the complexity of this pathway suggests that additional regulatory components may exist.

In our previous studies, compared transcriptomes of a green-leaf cultivar ('Dasusheng') and a purple-leaf cultivar ('Zixia'), identifying a previously uncharacterized *MYB* transcription factor, *LsMYB1* [19]. In this study, we through overexpression in the tobacco and CRISPR/Cas9-mediated gene editing to confirmed its role in regulating anthocyanin biosynthesis. These findings expand the regulatory network of anthocyanin accumulation in lettuce and provide potential molecular targets for breeding purple-leaf varieties with enhanced nutritional value.

2 Materials and Methods

2.1 Plant Materials

In this study, two lettuce (*Lactuca sativa* L.) cultivars, the green-leaf ('Dasusheng') and purple-leaf ('Zixia') lettuce plants were used (Fig. 1). Seeds of both cultivars were obtained from the Academy of Agriculture and Forestry, Qinghai University, Xining, China. The plants were cultivated at the experimental base of Qinghai University, Xining, China (36°43′6″ N, 101°45′15″ E). Three biological replicates were established for each cultivar. At approximately 30 days of growth, the leaf from the base of the stem was harvested for each replicate. Samples were immediately frozen in liquid nitrogen and stored at −80°C until use.

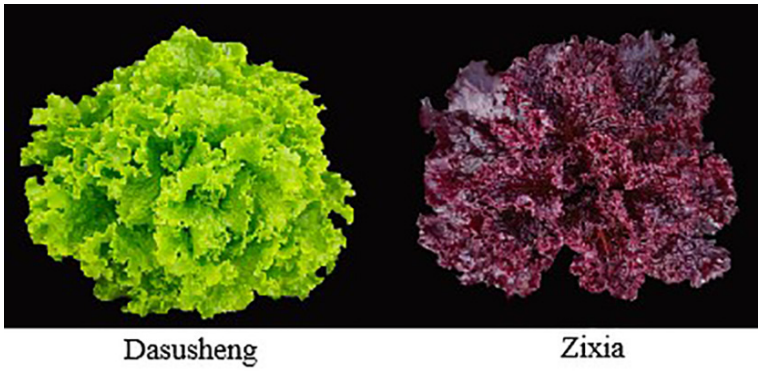

Figure 1: Plant materials.

2.2 Transcriptome Sequencing and Analysis

Transcriptome sequencing and data analysis were performed as previously described [19]. Total RNA was extracted using the TaKaRa MiniBEST Plant RNA Extraction Kit (Code No. 9769, TaKaRa, Japan). RNA integrity was assessed with an Agilent 2100 Bioanalyzer, and only samples with RIN $\geq$ 7.0 were used for library preparation. Sequenced on an Illumina NovaSeq 6000 platform (150 bp paired-end). Raw reads were trimmed with Fastp and aligned to the *L. sativa* reference genome (GCF_002870075.4) using HISAT2. DEGs were identified with DESeq2 ($|\log_2 FC| \geq 1$, FDR < 0.05), followed by GO and KEGG enrichment analyses.

2.3 Gene Cloning and Sequence Analysis

Genomic DNA and total RNA were obtainedfrom lettuce leaves using the TIANGEN Polysaccharide & Polyphenol Plant Genomic DNA Extraction Kit (TIANGEN, China) and the TaKaRa MiniBEST Plant RNA Extraction Kit (TaKaRa, Japan), respectively. According to the manufacturer's instructions, cDNA was generated from 1 μg of total RNA using the PrimeScript™ 1st Strand cDNA Synthesis Kit (TaKaRa, Japan). Using the primers LsMYB1-F and LsMYB1-R (refer to Table S1), we amplified both the complete genomic and coding sequences of *LsMYB1* from DNA and cDNA samples, respectively. The amplified products underwent examination through 1% agarose gel electrophoresis, werepurified by means of ethanol precipitation, and subsequently ligated into the pEASY-Blunt Zero vector using the pEASY-Blunt Zero Cloning Kit (TransGen Biotech, China). Following transformation into *E. coli* DH5α, Positive clones were detected via colony PCR (M13F/M13R; Table S1) and validated through Sanger sequencing (Sangon Biotech, Shanghai, China). Sequence alignment was carried out using Vector NTI Suite 11.5, while conserved domains were predicted withExPaSy-Protparam (http://expasy.org/tools/protparam.html), and aphylogenetic tree was created employing the neighbor-joining method in MEGA 11.

2.4 Analysis of LsMYB1 Expression by qRT-PCR

To examine the expression patterns specific to tissue types of *LsMYB1*, samples were obtained from the roots, stems, and leaves of 'Zixia' and 'Dasusheng' plants across three developmental phases: seedling, rosette, and mature stages. Total RNA isolation was conducted as outlined in Section 2.3, followed by the synthesis of first-strand cDNA. Quantitative real-time PCR (qRT-PCR) was executed employing 2 × ChamQ Universal SYBR qPCR Master Mix on a QuantStudioTM3Real-TimePCR system. The 18S rRNA gene from lettuce served as an internal reference to normalize expression levels (primer sequences are listed in Supplementary Table S1). Each sample consisted of three technical replicates and the relative expression levels of the gene were determined using the $2^{-\Delta\Delta CT}$ method.

2.5 Functional Analysis of LsMYB1 by Overexpression in Tobacco

2.5.1 Construction of the Overexpression Vector

To order to validate the function of *LsMYB1*, the pCAMBIA2300s vector was employedfor overexpression experiments in tobacco (*Nicotiana tabacum* cv. 'Samsun'). The CDS of *LsMYB1* was amplified through PCR, utilizing specific primers that incorporated KpnI and BamHI restriction sites (LsMYB1-KpnI-F/LsMYB1-BamHI-R, Table S1), with apreviously constructed recombinant plasmid serving as the template. The PCR product obtained was purified and subjected to double digestion alongside the pCAMBIA2300s vector using KpnI and BamHI (TaKaRa, Japan), followed by ligation with T4 DNA ligase (M0202S, New England Biolabs, USA). The resulting recombinant plasmid, named pCAMBIA2300s-LsMYB1, was transformed into E. coli DH5α by the heat shock method. Positive clones were then verified through colony PCR and DNA

sequencing (outlinedin Section 2.4). The verified plasmid was subsequently introduced into Agrobacterium tumefaciens strain GV3101 by applying the liquid nitrogen freeze-thaw method.

2.5.2 Stable Genetic Transformation of Tobacco

The tobacco transformation process was carried out the leaf disctechnique. Sterile leaf segments from 5-week-old Samsun seedlings were sliced into small pieces of approximately 1 cm^2 and placed in an Agrobacterium suspension (OD_{600} = 0.6–0.8) for a duration 10 min. Following infection, the explants were dried using sterile filter paper and then transferred to a co-cultivation medium, which consisted of MS medium supplemented with 1.0 mg/L 6-BA and 1 mg/L NAA, for 2 days in the dark. After co-cultivation period, the explants were moved to a shoot induction medium, which contained MS medium with1.0 mg/L 6-BA, 1.0 mg/L NAA, and 300 mg/L cefotaxime, and were subcultured every 2 weeks. Shoots that had regenerated to approximately 2 cm in height were cut and placed onto a rooting medium made from MS medium 1.0 mg/L NAA, 150 mg/L kanamycin and 300 mg/L cefotaxime. Theplantlets that developed roots were acclimatized and transplanted into soil. The presence of transgenic plants were verified through PCR with primers specific to the kanamycin resistance gene (LsMYB1-KpnI-F/LsMYB1-BamHI-R, Table S1). Wild-type (non-transformed) plants and water served as negative controls in the PCR evaluation.

2.5.3 qRT-PCR Analysis of Anthocyanin Pathway Genes

To investigate the expression variations of genes associated with anthocyanin biosynthesis in transgenic plants, total RNA was isolated from the leaves of both wild-type (WT) and transgenic tobacco lines, followed by qRT-PCR as detailed in Section 2.4. The NtActin gene served as the internal control (NtActin-qF/NtActin-qR, Table S1). Primers specific to key structural genes (*NtCHI*, *NtCHS*, *NtDFR*, *NtF3′5′H*, *NtF3H*, *NtANS*, *NtF3′H*) involved in the anthocyanin metabolic pathway were designed based on sequences derived from tobacco (Table S1). Each analysis included three biological replicates, and relative expression levels were calculated using the $2^{-\Delta\Delta CT}$ approach.

2.5.4 Anthocyanin Content Measurement

Anthocyanin content was measured using the pH method [20]. Anthocyanins were from fresh leaf tissue with acidified methanol (1% HCl) overnight at 4°C in the dark. The absorbance was measured at 525 nm and 700 nm after dilution in buffers of pH 1.0 and pH 4.5. The total anthocyanin content was calculated using the following formula:

$$\text{Anthocyanin content (mg/g FW)} = (A \times MW \times DF \times 1000)/\varepsilon \times 1$$

where $A = (A_{525nm} - A_{700nm})^{pH1.0} - (A_{525nm} - A_{700nm})^{pH4.5}$; MW is the molecular weight of cyanidin-3-glucoside (449.2 g/mol); DF is the dilution factor; 1000 is the extraction volume (mL); ε is the molar extinction coefficient of cyanidin-3-glucoside (26,900 L/mol·cm); l is the path length (1 cm).

2.6 CRISPR/Cas9-Mediated Gene Editing of LsMYB1 in Lettuce

2.6.1 Construction of the Dual-Target Gene Editing Vector

To further confirm the role of *LsMYB1*, a CRISPR/Cas9 system was employed to generate knockout mutants in purple-leaf (‘Zixia’) lettuce. Two sgRNA target sites, T1 and T2 (located in the first and third exons of *LsMYB1*, respectively), were designed using the CRISPOR online tool (https://crispor.gi.ucsc.edu/crispor.py) based on the presence of canonical NGG PAM motifs and high specificity scores (Fig. S1a). T1

spans nucleotides 8–29 of the *LsMYB1* coding sequence, and T2 spans nucleotides 884–905. Adapter primers for each target site (Table S2) were diluted to 10 μM, denatured at 90°C for 30 s, and then cooled to room temperature to form double-stranded DNA fragments (Fig. S1b).

These annealed adapters were ligated into the sgRNA scaffold using a Golden Gate reaction with BsaI-HF® v2 (NEB, R3733S) and T4 DNA ligase (NEB, M0202S) to connect the target sequences to the sgRNA scaffold. The sgRNA expression cassettes were then assembled via multi-round PCR using 2 × Phanta Flash Master Mix (Vazyme, P520). For T1, two first-round PCRs were performed to amplify the AtU3d promoter fused to the T1 spacer (fragment u1) and the T1 spacer fused to the sgRNA scaffold (fragment g1), respectively. The same strategy was applied to T2 to generate fragments u2 and g2. After verification by agarose gel electrophoresis, u1 and g1 were mixed and used as templates for a second-round PCR to fuse them into the complete AtU3-sgRNA1 expression cassette. Similarly, u2 and g2 were fused into the AtU6-sgRNA2 cassette. The detailed PCR conditions are provided in Fig. S1c,d.

Finally, the two sgRNA expression cassettes (AtU3-sgRNA1 and AtU6-sgRNA2) were assembled into the pYLCRISPR/Cas9P35S-H binary vector using a second Golden Gate reaction with BsaI-HF® v2 (NEB, R3733S) and T4 DNA ligase (NEB, M0202S), the complete experimental procedures are described in Fig. S1e. The resulting recombinant plasmid, designated as pYLCRISPR/Cas9-LsMYB1, was transformed into *E. coli* DH5α competent cells by the heat shock method. Positive clones were confirmed by colony PCR and Sanger sequencing. Detailed information on primers is available in Table S2.

2.6.2 Lettuce Genetic Transformation and Regeneration

The validated pYLCRISPR/Cas9-LsMYB1 plasmid was introduced into Agrobacterium tumefaciens strain GV3101 via the liquid nitrogen freeze-thaw method. Lettuce transformation was performed using the leaf disc method. Cotyledons from sterile seedlings of the purple-leaf cultivar 'Zixia' were excised, cut into small pieces (approximately 0.5 cm^2), pre-cultured for 1–2 days [MS medium supplemented with 0.5 mg/L KT, 0.3 mg/L IAA], and then immersed in the Agrobacterium suspension (OD_{600} = 0.3–0.5) for 10 min. The infected explants were blotted dry on sterile filter paper and transferred to co-cultivation medium [MS medium supplemented with 0.5 mg/L KT, 0.3 mg/L IAA, and 200 umol/L AS] for 2–3 days in the dark.

After co-cultivation, explants were transferred to shoot induction medium [MS medium containing 0.5 mg/L KT, 0.3 mg/L NAA,300 mg/L Timentin, and 10 mg/L Hyg] and subcultured every 2 weeks. Regenerated shoots (approximately 1–2 cm in height) were excised and transferred to rooting medium [1/2 MS medium containing 0.3 mg/L IAA and 300 mg/L Timentin]. Rooted plantlets were acclimatized and transplanted to soil for further analysis.

2.6.3 Identification of Transgenic Plants and Mutation Detection

Genomic DNA was extracted from leaves of wild-type (WT) and gene-edited lettuce lines using the super Plant Genomic DNA Kit (TIANGEN, China) according to the manufacture's instructions. Putative gene-editedplants were initially screened by PCR using *hygromycin phosphotransferase* (Hyg) gene-specific primers (Table S2). To characterize the mutations induced by CRISPR/Cas9, genomic regions flanking the T1 and T2 target sites were amplified by PCR using Hi-TOM sequencing primers (Table S2), and the products were subjected to Hi-TOM high-throughput sequencing to analyze the mutation patterns at the target sites. The phenotypic changes in gene-edited plants, particularly leaf coloration and anthocyanin accumulation, were observed and documented.

2.6.4 Expression Analysis of Anthocyanin Pathway Genes

To assess the impact of *LsMYB1* knockout on the anthocyanin biosynthetic pathway, total RNA was extracted from leaves of wild-type (WT) and gene-edited lettuce lines, and qRT-PCR was performed using a QuantStudio^{TM} 3 Real-Time PCR System with gene-specific primers for key structural genes involved in anthocyanin biosynthesis (*CHI*, *CHS*, *DFR*, *F3′5′H*, *F3H*) and the internal reference gene (18S rRNA) (Table S2). Each sample included three biological replicates, and relative expression levels were calculated using the $2^{-\Delta\Delta CT}$ method.

3 Results

3.1 Identification of LsMYB1 as a Candidate Gene

In our previous transcriptome analysis between the purple-leaf cultivar 'Zixia' and the green-leaf cultivar 'Dasusheng', a *MYB* transcription factor gene (LOC111917799) was identified as a candidate regulator of anthocyanin biosynthesis, showing 5.56-fold higher expression in the purple cultivar [19]. This gene was designated *LsMYB1* and selected for further functional validation in the present study.

3.2 Cloning and Sequence Analysis of LsMYB1

The genomic and coding sequences of *LsMYB1* were cloned from both lettuce cultivars. Sequence analysis revealed marked structural differences between the two alleles. In the purple cultivar 'Zixia', the *LsMYB1* gene spanned 1374 bp and comprised two introns and three exons, with a coding sequence (CDS) of 759 bp. In contrast, the allele from the green cultivar 'Dasusheng' was 759 bp in length and consisted of a single exon with no introns (Fig. 2A). This structural variation may contribute to the differential expression of *LsMYB1* observed between the two cultivars.

The *LsMYB1* protein, deduced from the 'Zixia' allele, consists of 252 amino acids. Multiple sequence alignment demonstrated that *LsMYB1* including two SANT domains (13–60 and 15–62) and a MYB-DNA binding domain (66–111), and shares high sequence conservation in the R3 domain with *MYB* proteins from other Asteraceae species and contains the 'ANDV' motif, which is specific to dicotyledonous *MYB* transcription factors involved in anthocyanin regulation (Fig. 2B). Phylogenetic tree was constructed using *MYB* proteins from different plant species. The results showed that these *MYB* proteins were divided into four major groups (Groups A–D). *LsMYB1* clustered together with several reported anthocyanin-related MYB transcription factors, including *HaMYB1* [21], *HtMYB2* [22]. The close phylogenetic relationship between *LsMYB1* and these anthocyanin-associated MYBs suggests that *LsMYB1* may play a conserved role in regulating anthocyanin biosynthesis in lettuce (Fig. 2C). This phylogenetic relationship further supports the putative role of *LsMYB1* in regulating anthocyanin biosynthesis.

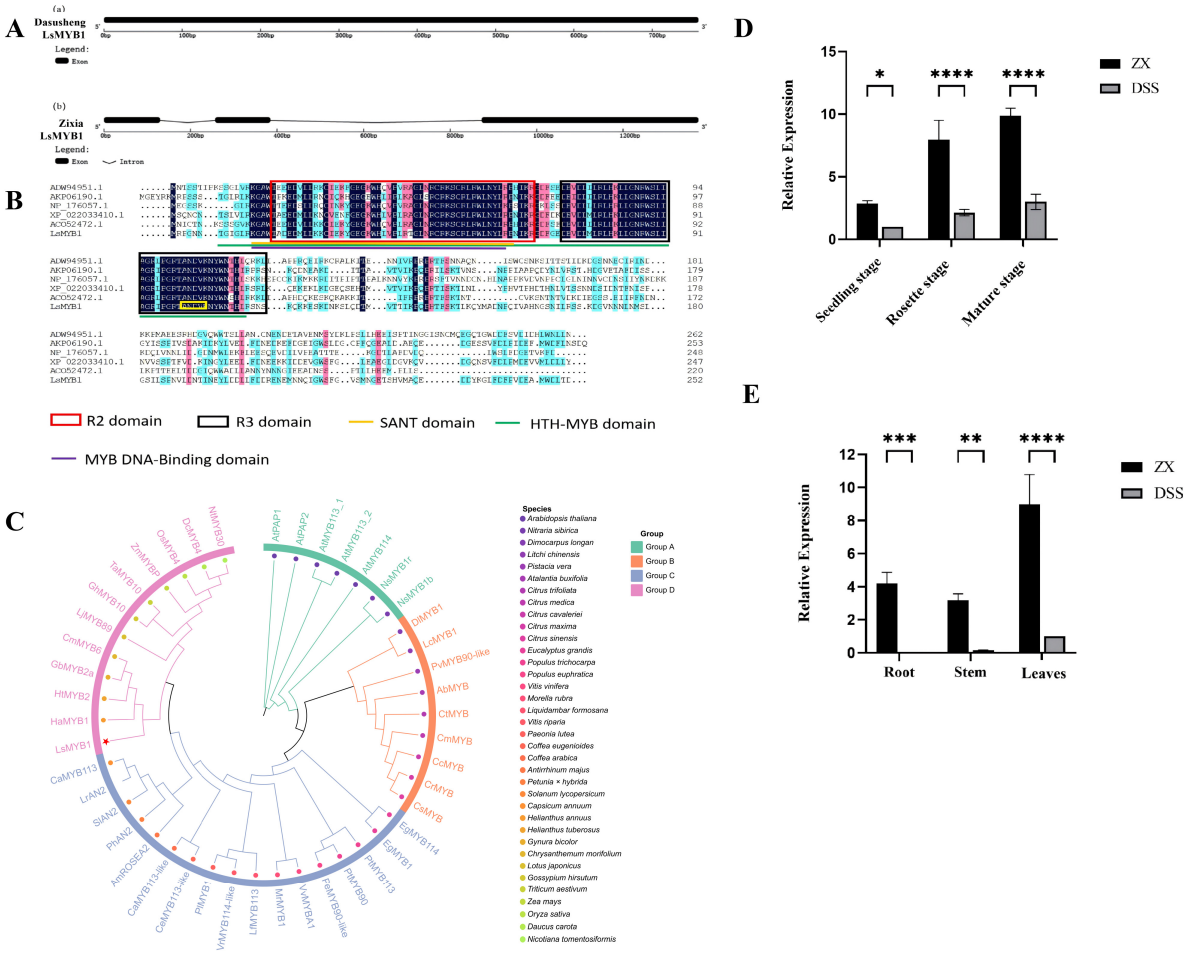

Figure 2: Gene Cloning and Sequence Analysis. (**A**) Structure diagram of the *LsMYB1* gene, (a) Gene structure of 'Dasushen' *LsYMB1.* (b) Gene structure of 'Zixia' *LsYMB1.* (**B**) Domain prediction. (**C**) Phylogenetic analysis, the detailed sequence information is provided in Fig. S2. (**D**) Analysis of the expression levels of the *LsMYB1* at different growth stages Phylogenetic Analysis. (**E**) Expression analysis of *LsMYB1* in different tissues. $^{*}p < 0.05$; $^{**}p < 0.01$; $^{***}p < 0.001$; $^{****}p < 0.0001$.

3.3 Expression Patterns of LsMYB1

Quantitative real-time PCR (qRT-PCR) analysis revealed distinct expression patterns of *LsMYB1* between the two lettuce cultivars. In the purple cultivar 'Zixia', *LsMYB1* transcript levels increased progressively with plant development, with the lowest expression detected at the seedling stage and the highest at the mature stage across all tissues examined (Fig. 2D). Tissue-specific analysis showed that *LsMYB1* was predominantly expressed in leaves, with significantly higher transcript levels than in roots and stems at all three developmental stages ($p < 0.01$; Fig. 2E). This leaf-preferential and developmentally regulated expression pattern of *LsMYB1* is consistent with the anthocyanin accumulation phenotype observed in the purple-leaf cultivar 'Zixia'.

3.4 Overexpression of LsMYB1 in Tobacco

3.4.1 Generation and Early Phenotypic Observation of Transgenic Lines

Stable transgenic tobacco lines overexpressing *LsMYB1* were generated via Agrobacterium-mediated transformation. Approximately 50 days after infection, most transformed calli turned purple, indicating early transgene expression (Fig. 3A). Around 70 days after infection, some regenerated shoots developed purple sectors on their leaves, which gradually intensified during subsequent growth on rooting medium.

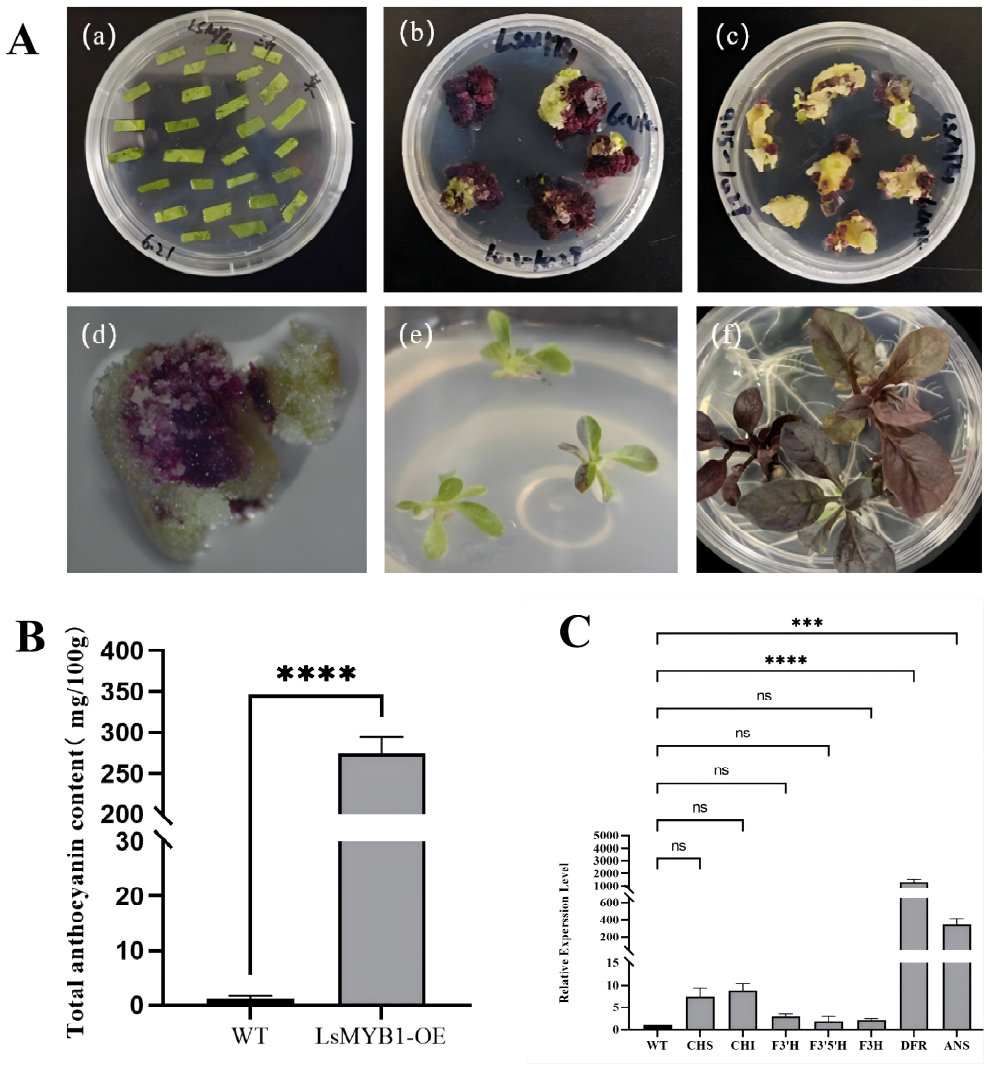

Figure 3: Analysis of Overexpression Effects. (**A**) Genetic Transformation of Lettuce. (a) Infiltration of tobacco leaves. (b) Induction of callus formation. (c) Differentiation of shoots. (d) High-magnification stereomicroscopic view of callus tissue (imaged using a T2-HD206 stereomicroscope). (e) Rooting culture. (f) Regeneration of transgenic plantlets. (**B**) Comparative Analysis of Anthocyanin Content in WT and Transgenic Plants. (**C**) Expression Analysis of Key Genes in Anthocyanin Biosynthesis. $^{***}p < 0.001$; $^{****}p < 0.0001$; ns indicates not significant ($p \geq 0.05$).

3.4.2 Molecular Confirmation of Transgenic Plants

To confirm the transgenic regenerated plants, genomic DNA was extracted from leaves and subjected to PCR analysis using *LsMYB1*-specific primers (Table S1). The expected fragment was amplified from all

selected lines showing the purple phenotype, whereas no amplification was observed in wild-type plants, confirming the successful integration of the transgene.

3.4.3 Anthocyanin Accumulation in Transgenic Plants

Quantitative revealed that anthocyanin content in transgenic plants reached 273.56 ± 20.64 mg/100 g fresh weight, which was significantly higher than that in wild-type plants (1.16 ± 0.53 mg/100 g), representing an approximately 236-fold increase ($p < 0.0001$; Fig. 3B).

3.4.4 Expression Analysis of Anthocyanin Biosynthetic Genes

To further explore the molecular mechanism underlying *LsMYB1*-mediated anthocyanin accumulation, the expression levels of key structural genes in the anthocyanin biosynthetic pathway were examined by quantitative real-time PCR (qRT-PCR). In *LsMYB1*-overexpressing lines, all tested structural genes were significantly up-regulated compared with wild-type plants. Notably, the transcript levels of *DFR* and *ANS* showed the most dramatic increases; the relative expression of *DFR* (1300.78 ± 178.70) was approximately 1300-fold higher than that in the wild type ($p < 0.0001$; Fig. 3C). These results suggest that *LsMYB1* promotes anthocyanin accumulation, at least in part, by activating the expression of key downstream genes in the anthocyanin biosynthetic pathway.

3.5 Functional Validation of LsMYB1 by CRISPR/Cas9 Gene Editing

3.5.1 Confirmation of the Dual-Target CRISPR/Cas9 Vector

Based on the designed target sites (T1 and T2), adapter primers were designed. Using the digestion–ligation product as a template, first-round PCR was performed to generate target sequence-containing fragments: u1 (200 bp) and g1 (150 bp) for T1, and u2 (500 bp) and g2 (150 bp) for T2. The sgRNA fragments were then fused with the AtU3 and AtU6 promoters via second-round PCR, yielding fragments 6-T1 (250 bp) and 6-T2 (450 bp) (Fig. 4A). These fragments were assembled into the sgRNA vector by Golden Gate ligation to construct intermediate vectors for the two target sites. After confirmation, the constructs were used for subsequent applications. Positive clones were identified by colony PCR and Sanger sequencing (Fig. S1f).

3.5.2 Generation and Phenotypic Characterization of LsMYB1-Edited Lettuce Lines

Through *Agrobacterium*-mediated genetic transformation, a total of 2 independent LsMYB1-edited lettuce lines were successfully generated. PCR analysis using *hygromycin phosphotransferase (Hyg)* gene-specific primers confirmed the presence of the selection marker in the putative edited lines, whereas no amplification was detected in wild-type plants (Fig. S1g).

Phenotypically, wild-type plants exhibited uniformly deep purple leaves. In contrast, the two gene-edited lines showed a striking reduction in anthocyanin accumulation, with pigmentation restricted to narrow regions along the leaf margins, while most of the leaf surface appeared green, similar to green-leaf germplasm (Fig. 4B,C). These results confirmed the successful generation of *LsMYB1*-edited lettuce lines with altered pigmentation.

3.5.3 Molecular Characterization of Editing Events

Hi-TOM sequencing of T0 edited plants revealed a single thymine (T) insertion at the first target site (T1) of *LsMYB1* in one of the edited lines, resulting in a frameshift mutation (Fig. 4D). This mutation altered the downstream amino acid sequence and introduced a premature stop codon (TGA) at position 82, resulting in a truncated *LsMYB1* protein of approximately 81 amino acids (compared to 252 aa in the wild

type) and likely disrupting the conserved MYB DNA-binding domain (Fig. 4E). These results indicate that the CRISPR/Cas9-induced mutation severely impaired the normal function of *LsMYB1*.

3.5.4 Anthocyanin Content in Edited Plants

Total anthocyanin content was measured by the pH differential method. WT plants had 297.66 ± 6.85 mg/100 g FW, while edited plants had 73.92 ± 4.00 mg/100 g FW, a 75.2% reduction ($p < 0.001$). These results provide physiological evidence that *LsMYB1* plays a central role in regulating anthocyanin biosynthesis (Fig. 4F).

3.5.5 Expression Analysis of Anthocyanin Biosynthetic Genes in LsMYB1-Edited Lettuce

To further investigate the impact of *LsMYB1* knockout on anthocyanin biosynthetic structural genes, quantitative real-time PCR (qRT-PCR) was performed to analyze the expression levels of these genes in wild-type purple-leaf lettuce and the edited line. The results showed that the expression levels of all detected anthocyanin biosynthetic structural genes were significantly lower in the edited line than in the wild type, with *DFR* showing the most pronounced decrease (77-fold) (Fig. 4G).

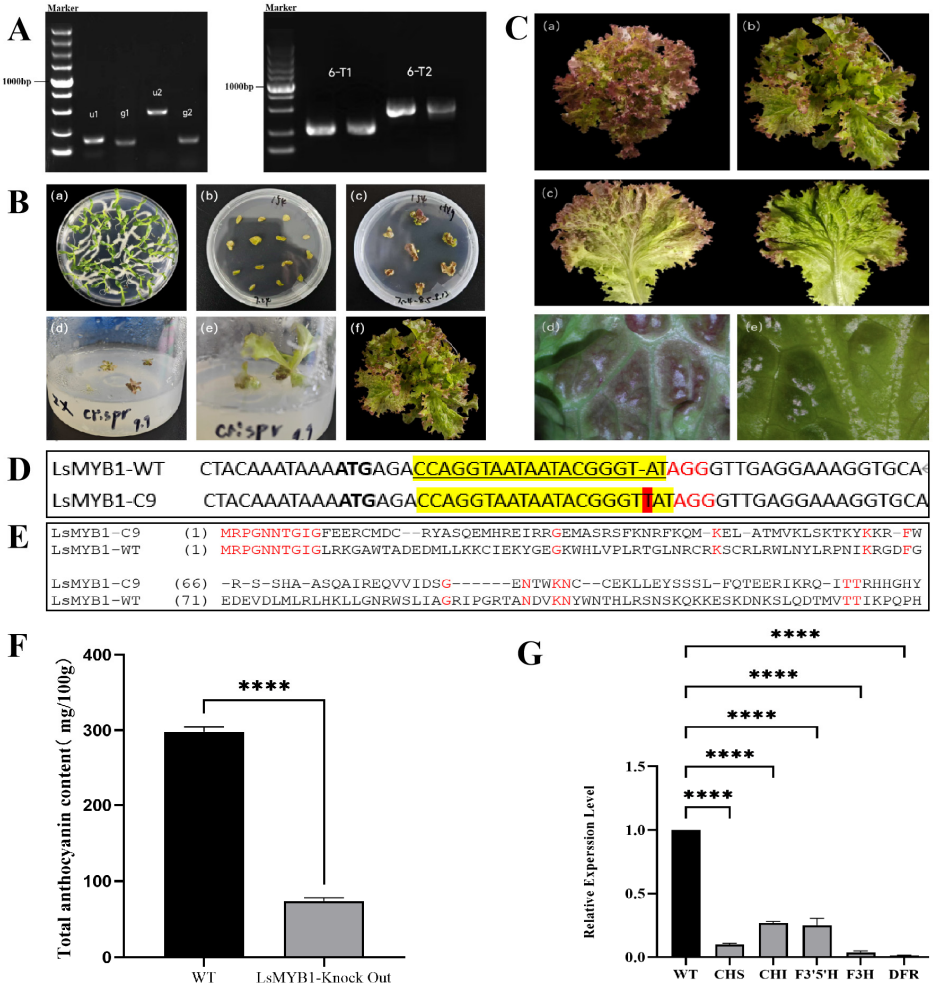

Figure 4: Validation of CRISPR/Cas9-Mediated Gene Editing. (**A**) Verification of Vector Construction by Gel Electrophoresis. (**B**) Plant Transformation and Regeneration for CRISPR/Cas9 Gene Editing. (a) Sterile leaf lettuce seedlings. (b) Agrobacterium-mediated transformation of leaf explants. (c) Callus induction and adventitious shoot

regeneration. (d) Rooting culture. (e) Root development in regenerated plantlets. (f) Transgenic leaf lettuce plants. (**C**) Phenotypic Variation in Positive Transformants. (a) Wild-type plant. (b) Gene-edited plant. (c) Leaf phenotype comparison: wild-type (left) vs. gene-edited (right). (d) Magnified view of wild-type leaf under a T2-HD206 stereomicroscope. (e) Magnified view of gene-edited leaf under a T2-HD206 stereomicroscope. (**D**) Genotyping of Mutation Types at the Target Locus. (**E**) Translation and Alignment of Amino Acid Sequences from Edited Alleles. (**F**) Comparative Analysis of Anthocyanin Content in WT and CRISPR/Cas9-Edited Plants. (**G**) Expression Analysis of Key Genes in Anthocyanin Biosynthesis. $^{****}p < 0.0001$.

4 Discussion

4.1 Structural Variation of LsMYB1

As a key family of transcription factors, *MYB* proteins are extensively implicated in the regulation of plant secondary metabolism and play an essential role in anthocyanin biosynthesis [23–25].

A key finding of this study is the structural difference in the *LsMYB1* gene between the two cultivars. The purple-leaf allele has two introns and three exons, while the green-leaf allele consists of a single exon (Fig. 3a,b). The presence of introns in the purple-leaf allele correlates with significantly higher *LsMYB1* expression and anthocyanin accumulation, suggesting that these introns may positively regulate gene expression. This observation aligns with the concept of intron-mediated enhancement (IME), whereby introns can enhance transcription efficiency, mRNA stability, and nuclear export, thereby boosting gene expression [26]. Similar phenomena have been observed in other plants species. For instance, intron variation in apple *MMK2* affects skin coloration [27]. Phylogenetic analysis confirmed that *LsMYB1* clusters with functionally validated MYB proteins from other Asteraceae species [28,29]. *LsMYB1* likely functions as the *MYB* component of the conserved MBW complex in lettuce, promoting anthocyanin biosynthesis [30] Nevertheless, whether the intron present in the purple-leaf *LsMYB1* allele directly affects its expression and regulatory function remains to be further investigated.

4.2 LsMYB1 Positively Regulates Anthocyanin Biosynthesis

In *Arabidopsis*, overexpression of the *AtMYB75* gene upregulates the expression of structural genes involved in the anthocyanin biosynthetic pathway, leading to anthocyanin accumulation [31]. Purple coneflower (Echinacea purpurea), a member of the Asteraceae family, contains the transcription factor *EpMYB1*, which positively regulate anthocyanin biosynthesis by upregulating anthocyanin-specific biosynthetic genes [32]. In sunflower flowers, the transcription factor *HaMYB1* promotes anthocyanin accumulation in red sunflowers by directly activating *UFGT* expression [33]. *AtMYB60* functions as a transcriptional repressor of anthocyanin biosynthesis in lettuce, whereas *LsMYB1* acts as a positive regulator. In this study, we further characterized *LsMYB1*, a previously identified *MYB* transcription factor, and demonstrated its role as a positive regulator of anthocyanin biosynthesis in purple-leaf lettuce. However, functional redundancy among *MYB* transcription factors may exist in the lettuce anthocyanin pathway. The regulation of anthocyanin biosynthesis involves sophisticated feedback loops. In Arabidopsis, an *R3-MYB* repressor *MYBL2* and an *R2R3-MYB* activator *PAP1* form a negative feedback regulatory module that fine-tunes high light-induced anthocyanin biosynthesis [34,35].

The present study has several limitations regarding the scope of gene expression analysis. In the overexpression tobacco lines, qRT-PCR analysis focused primarily on the core structural genes (*CHS*, *CHI*, *F3H*, *DFR*, *ANS*), while key downstream genes such as *UFGT*, which catalyzes the final step of anthocyanin stabilization, and the transporter genes *GST* and *MATE*, which are responsible for vacuolar sequestration, were not examined. Similarly, in the *LsMYB1*-edited lettuce lines, the expression analysis was limited to a

subset of structural genes (*CHI*, *CHS*, *DFR*, *F3′H*, *F3H*), and did not include *ANS*, *UFGT*, or the transporter genes *GST* [36]. In addition, the lack of metabolite quantification at the exact time point of transcriptome analysis is a limitation of the present study [37]. Despite these limitations, recent studies have highlighted the critical roles of these genes in anthocyanin biosynthesis. A comprehensive review emphasizes the importance of various decorating enzymes and transporters in anthocyanin modification and accumulation [38]. Moreover, anthocyanin-related glutathione S-transferases (*arGSTs*) play a catalytic role in the conversion of leucoanthocyanidins to anthocyanidins, rather than merely acting as transporters. Their study showed that inclusion of *arGSTs* in a heterologous yeast system boosted anthocyanin production by up to 36.5-fold [39]. Therefore, whether *LsMYB1* also regulates the expression of *UFGT*, *GST*, *MATE*, and other decorating enzyme genes remains an open question that warrants further investigation. Future studies should expand the qRT-PCR analysis to include these missing genes to fully elucidate the regulatory network downstream of *LsMYB1*.

4.3 Breeding Implications and Future Directions

Anthocyanins provide various health benefits to humans, which has led to the increasing popularity of anthocyanin-rich foods among consumers. Lettuce, as a prominent leafy vegetable, serves as an ideal candidate for the development of anthocyanin-rich varieties. In our previous study, we identified LsMYB1 as a crucial regulator of anthocyanin biosynthesis through transcriptome analysis [19]. In the current study, we further validated its function through overexpression in tobacco and CRISPR/Cas9-mediated gene editing in lettuce. The successful implementation of CRISPR/Cas9 highlights the feasibility of genome editing in lettuce and presents a promising target for breeding varieties with enhanced nutritional value. Furthermore, the structural variations identified in this study may act as molecular markers for marker-assisted selection.

5 Conclusion

LsMYB1 functions as a positive regulator of anthocyanin biosynthesis in leaf lettuce. Sequence analysis revealed structural variation between the two alleles (the purple allele contains two introns and three exons, while the green allele is intronless), which may account for their differential expression. The gene exhibits a 5.56-fold higher expression level in the purple cultivar ‘Zixia’ compared to the green cultivar ‘Dasusheng’. Sequence analysis has revealed structural variations between the two alleles, which may account for their differential expression. Functional validation through overexpression in tobacco resulted in a significant increase in anthocyanin content (236-fold) and the activation of key biosynthetic genes, particularly DFR, which was upregulated by 1300-fold. Conversely, CRISPR/Cas9-mediated knockout of *LsMYB1* in lettuce led to a marked reduction in pigmentation. Collectively, these findings position *LsMYB1* as a crucial regulator of anthocyanin metabolism and highlight its potential as a target for breeding lettuce varieties with enhanced nutritional value.

Acknowledgement: We are grateful to the research group of Professor Liu Baolong from the Northwest Institute of Plateau Biology, Chinese Academy of Sciences.

Funding Statement: This work was supported by the Qinghai Province application foundation [2025-ZJ-968T].

Author Contributions: The authors confirm contribution to the paper as follows: writing—review and editing Xuebing Zhu; Data curation, Yongqiang Jiang; Writing—review & editing, Wei Li; Visualization, Lihui Wang; Conceptualization and Funding acquisition, Xuemei Sun. All authors reviewed and approved the final version of the manuscript.

Availability of Data and Materials: All raw data were uploaded in the Genome Sequence Archive at the Big Data Center, Beijing Institute of Genomics, Chinese Academy of Sciences, accession numbers CRA041092 (https://ngdc.cncb.ac.cn).

Ethics Approval: Not applicable.

Conflicts of Interest: The authors declare no conflicts of interest.

Supplementary Materials: The supplementary material is available online at https://www.techscience.com/doi/10.32604/phyton.2026.083772/s1.

References

1. Huo H, Dahal P, Kunusoth K, McCallum CM, Bradford KJ. Expression of *9-cis-EPOXYCAROTENOID DIOXYGENASE4* is essential for thermoinhibition of lettuce seed germination but not for seed development or stress tolerance. Plant Cell. 2013;25(3):884–900. [CrossRef].
2. Ismail H, Gillespie AL, Calderwood D, Iqbal H, Gallagher C, Chevallier OP, et al. The health promoting bioactivities of *Lactuca sativa* can be enhanced by genetic modulation of plant secondary metabolites. Metabolites. 2019;9(5):97. [CrossRef].
3. Zhang Q, Zhang X, Wu Y, Li X. TMSCNet: A three-stage multi-branch self-correcting trait estimation network for RGB and depth images of lettuce. Front Plant Sci. 2022;13:982562. [CrossRef].
4. Du J, Lu X, Fan J, Qin Y, Yang X, Guo X. Image-based high-throughput detection and phenotype evaluation method for multiple lettuce varieties. Front Plant Sci. 2020;11:563386. [CrossRef].
5. Deng H, Kong Y, Zhu J, Jiao X, Tong Y, Wan M, et al. Proteomic analyses revealed the antibacterial mechanism of *Aronia melanocarpa* isolated anthocyanins against *Escherichia coli* O157: H7. Curr Res Food Sci. 2022;5:1559–69. [CrossRef].
6. Leonardou VK, Doudoumis E, Tsormpatsidis E, Vysini E, Papanikolopoulos T, Papasotiropoulos V, et al. Quality traits, volatile organic compounds, and expression of key flavor genes in strawberry genotypes over harvest period. Int J Mol Sci. 2021;22(24):13499. [CrossRef].
7. Luo Y, Teng S, Yin H, Zhang S, Tuo X, Tran LP. Transcriptome analysis reveals roles of anthocyanin- and jasmonic acid-biosynthetic pathways in rapeseed in response to high light stress. Int J Mol Sci. 2021;22(23):13027. [CrossRef].
8. Cao X, Hu Y, Song J, Feng H, Wang J, Chen L, et al. Transcriptome sequencing and metabolome analysis reveals the molecular mechanism of drought stress in millet. Int J Mol Sci. 2022;23(18):10792. [CrossRef].
9. Li J, Han G, Sun C, Sui N. Research advances of MYB transcription factors in plant stress resistance and breeding. Plant Signal Behav. 2019;14(8):1613131. [CrossRef].
10. Zhang Q, Zhai J, Shao L, Lin W, Peng C. Corrigendum: Accumulation of anthocyanins: An adaptation strategy of *Mikania micrantha* to low temperature in winter. Front Plant Sci. 2019;10:1796. [CrossRef].
11. Ceci AT, Franceschi P, Serni E, Perenzoni D, Oberhuber M, Robatscher P, et al. Metabolomic characterization of pigmented and non-pigmented potato cultivars using a joint and individual variation explained (JIVE). Foods. 2022;11(12):1708. [CrossRef].
12. Sun C, Wang C, Zhang W, Liu S, Wang W, Yu X, et al. The R2R3-type MYB transcription factor MdMYB90-like is responsible for the enhanced skin color of an apple bud sport mutant. Hortic Res. 2021;8:156. [CrossRef].
13. Van Brenk JB, Courbier S, Kleijweg CL, Verdonk JC, Marcelis LFM. Corrigendum: Paradise by the far-red light: Far-red and red: Blue ratios independently affect yield, pigments, and carbohydrate production in lettuce, *Lactuca sativa*. Front Plant Sci. 2024;15:1442349. [CrossRef].
14. Zhang Y, Xu S, Cheng Y, Peng Z, Han J. Transcriptome profiling of anthocyanin-related genes reveals effects of light intensity on anthocyanin biosynthesis in red leaf lettuce. PeerJ. 2018;6:e4607. [CrossRef].
15. Kameniarová M, Černý M, Novák J, Ondrisková V, Hrušková L, Berka M, et al. Light quality modulates plant cold response and freezing tolerance. Front Plant Sci. 2022;13:887103. [CrossRef].
16. Su W, Tao R, Liu W, Yu C, Yue Z, He S, et al. Characterization of four polymorphic genes controlling red leaf colour in lettuce that have undergone disruptive selection since domestication. Plant Biotechnol J. 2020;18(2):479–90. [CrossRef].

17. Zhang L, Su W, Tao R, Zhang W, Chen J, Wu P, et al. RNA sequencing provides insights into the evolution of lettuce and the regulation of flavonoid biosynthesis. Nat Commun. 2017;8(1):2264. [CrossRef].
18. Tao R, Ma J, Qian J, Liu Y, Zhang W, Lavelle D, et al. Differential methylation of a retrotransposon upstream of a *MYB* gene causes variegation of lettuce leaves, which is abolished by the presence of an $(AT)_5$ repeat in the promoter. Plant J. 2025;122:e70123. [CrossRef].
19. Jiang Y, Wang L, Sun X. Identification of key genes involved in anthocyanin biosynthesis in *Lactuca sativa* L. based on transcriptome analysis. Jiangsu J Agric Sci. 2025;41(1):150–60. (In Chinese). [CrossRef].
20. Kanpipit N, Nualkaew N, Kiatponglarp W, Priprem A, Thapphasaraphong S. Development of a sericin hydrogel to deliver anthocyanins from purple waxy corn cob (*Zea mays* L.) extract and *in vitro* evaluation of anti-inflammatory effects. Pharmaceutics. 2022;14(3):577. [CrossRef].
21. Ma X, Zhang Q, Zhu Q, Liu W, Chen Y, Qiu R, et al. A robust CRISPR/Cas9 system for convenient, high-efficiency multiplex genome editing in monocot and dicot plants. Mol Plant. 2015;8(8):1274–84. [CrossRef].
22. Gao J, Sun X, Zong Y, Yang S, Wang L, Liu B. Functional *MYB* transcription factor gene HtMYB2 is associated with anthocyanin biosynthesis in *Helianthus tuberosus* L. BMC Plant Biol. 2020;20(1):247. [CrossRef].
23. Wu X, Xia M, Su P, Zhang Y, Tu L, Zhao H, et al. MYB transcription factors in plants: A comprehensive review of their discovery, structure, classification, functional diversity and regulatory mechanism. Int J Biol Macromol. 2024;282(Pt 2):136652. [CrossRef].
24. Yang J, Chen Y, Xiao Z, Shen H, Li Y, Wang Y. Multilevel regulation of anthocyanin-promoting R2R3-MYB transcription factors in plants. Front Plant Sci. 2022;13:1008829. [CrossRef].
25. Huang G, Liao X, Han Q, Zhou Z, Liang K, Li G, et al. Integrated metabolome and transcriptome analyses reveal dissimilarities in the anthocyanin synthesis pathway between different developmental leaf color transitions in *Hopea hainanensis* (Dipterocarpaceae). Front Plant Sci. 2022;13:830413. [CrossRef].
26. Shaul O. How introns enhance gene expression. Int J Biochem Cell Biol. 2017;91:145–55. [CrossRef].
27. Wang T, Duan S, Xu C, Wang Y, Zhang X, Xu X, et al. Pan-genome analysis of 13 *Malus* accessions reveals structural and sequence variations associated with fruit traits. Nat Commun. 2023;14(1):7377. [CrossRef].
28. Li J, Liu H, Yang C, Wang J, Yan G, Si P, et al. Genome-wide identification of *MYB* genes and expression analysis under different biotic and abiotic stresses in *Helianthus annuus* L. Ind Crops Prod. 2020;143:111924. [CrossRef].
29. Shimizu Y, Maeda K, Kato M, Shimomura K. Co-expression of *GbMYB1* and *GbMYC1* induces anthocyanin accumulation in roots of cultured *Gynura bicolor* DC. plantlet on methyl jasmonate treatment. Plant Physiol Biochem. 2011;49(2):159–67. [CrossRef].
30. Zhu T, Du M, Chen H, Li G, Wang M, Meng L. Recent insights into anthocyanin biosynthesis, gene involvement, distribution regulation, and domestication process in rice (*Oryza sativa* L.). Plant Sci. 2024;349:112282. [CrossRef].
31. Borevitz JO, Xia Y, Blount J, Dixon RA, Lamb C. Activation tagging identifies a conserved *MYB* regulator of phenylpropanoid biosynthesis. Plant Cell. 2000;12(12):2383–94. [CrossRef].
32. Jin G, Deng Z, Wang H, Li W, Su L, Zhang Y, et al. A stress-responsive R2R3-MYB transcription factor, EpMYB1 is involved in the regulation of anthocyanin biosynthesis in purple coneflower. Ind Crops Prod. 2024;209:118043. [CrossRef].
33. Ma S, Zhou H, Ren T, Yu ER, Feng B, Wang J, et al. Integrated transcriptome and metabolome analysis revealed that HaMYB1 modulates anthocyanin accumulation to deepen sunflower flower color. Plant Cell Rep. 2024;43(3):74. [CrossRef].
34. Park JS, Kim JB, Cho KJ, Cheon CI, Sung MK, Choung MG, et al. *Arabidopsis* r2r3-MYB transcription factor AtMYB60 functions as a transcriptional repressor of anthocyanin biosynthesis in lettuce (*Lactuca sativa*). Plant Cell Rep. 2008;27(6):985–94. [CrossRef].
35. Xing M, Xin P, Wang Y, Han C, Lei C, Huang W, et al. A negative feedback regulatory module comprising R3-MYB repressor MYBL2 and R2R3-MYB activator PAP1 fine-tunes high light-induced anthocyanin biosynthesis in *Arabidopsis*. J Exp Bot. 2024;75(22):7381–400. [CrossRef].
36. Li C, Yu W, Xu J, Lu X, Liu Y. Anthocyanin biosynthesis induced by *MYB* transcription factors in plants. Int J Mol Sci. 2022;23(19):11701. [CrossRef].
37. Pucker B, Brockington SF. The evidence for anthocyanins in the betalain-pigmented genus *Hylocereus* is weak. BMC Genom. 2022;23(1):739. [CrossRef].

38. Grünig N, Horz JM, Pucker B. Diversity and ecological functions of anthocyanins. BMC Plant Biol. 2025;26(1):146. [CrossRef].
39. Eichenberger M, Schwander T, Hüppi S, Kreuzer J, Mittl PRE, Peccati F, et al. The catalytic role of glutathione transferases in heterologous anthocyanin biosynthesis. Nat Catal. 2023;6(10):927–38. [CrossRef].